Electronic Supplementary Material (ESI) for Physical Chemistry Chemical Physics

ELECTRONIC SUPPLEMENTARY INFORMATION

PHENOL TRANSFORMATION PHOTOSENSITISED BY QUINOID COMPOUNDS

Valter Maurino,[a] Andrea Bedini,[a] Daniele Borghesi,[a] Davide Vione,[a,b,*] Claudio Minero[a,*]

[a] *Dipartimento di Chimica Analitica, Università di Torino, Via P. Giuria 5, 10125 Torino, Italy. http://www.chimicadellambiente.unito.it*

[b] *Centro Interdipartimentale NatRisk, Università di Torino, Via Leonardo Da Vinci 44, 10095 Grugliasco (TO), Italy.*

* Corresponding authors. Fax +39-011-6707615 E-mail: *claudio.minero@unito.it davide.vione@unito.it*

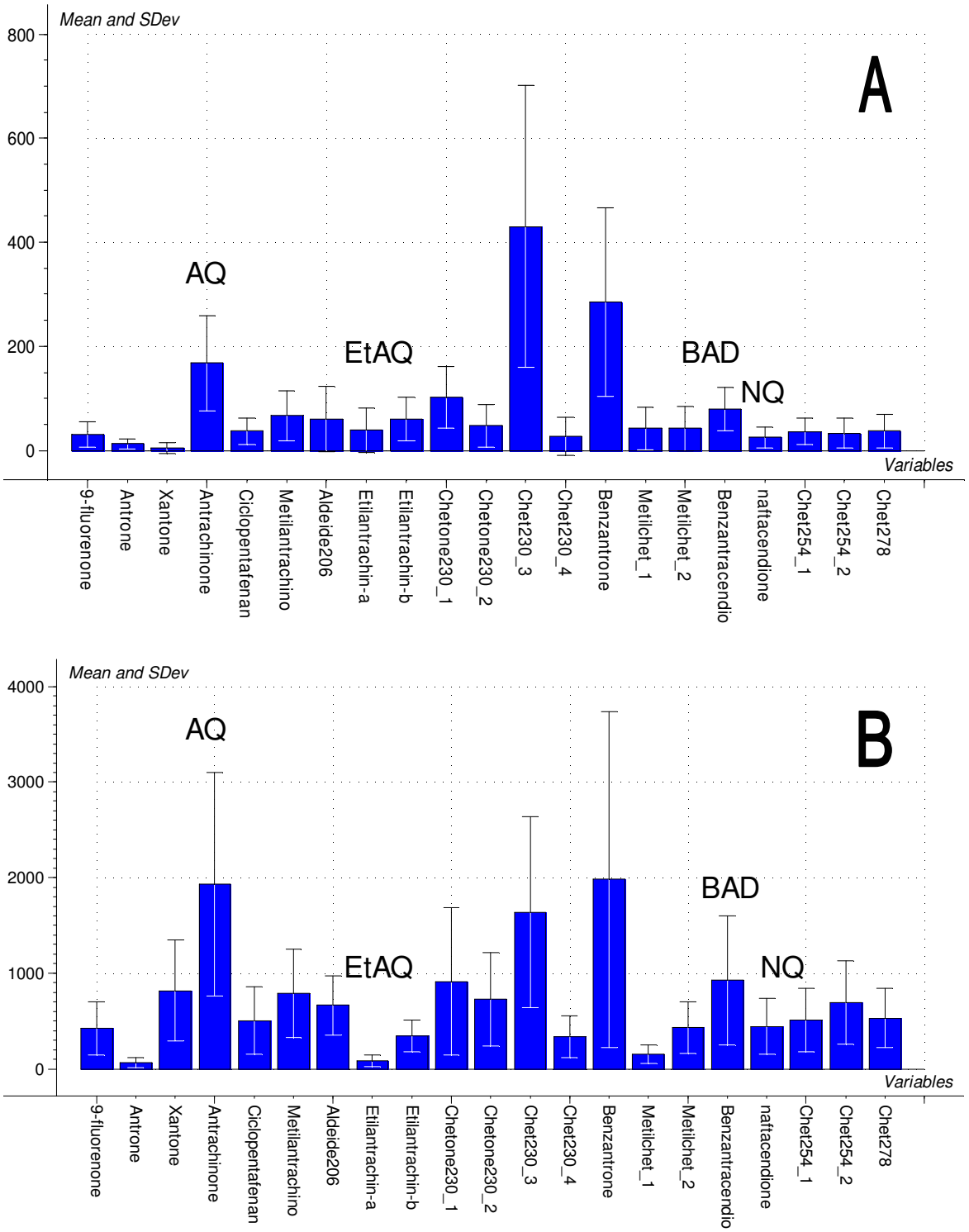

Figure ESI1. Oxygenated polyaromatic compounds detected on atmospheric particulate matter in the province of Torino (NW Italy), in summer (A) and winter (B) sampling campaigns. The compounds investigated in the present study are highlighted. Note that two ethylanthraquinone isomers have been detected on particulate matter. Units are arbitrary, derived from chromatographic peak areas.

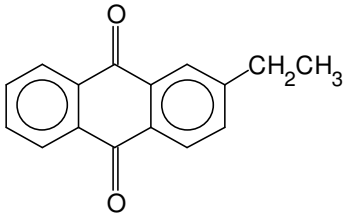

2-Ethylanthraquinone (**EtAQ**)

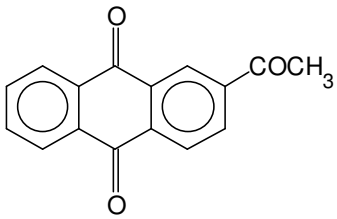

2-(1-Oxoethyl)anthraquinone

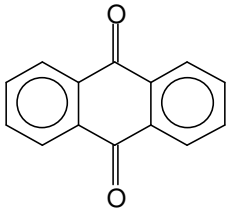

9,10-Anthraquinone (**AQ**)

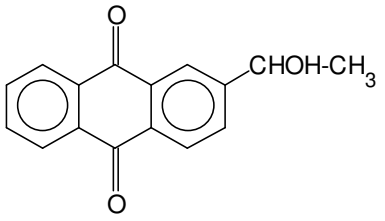

2-(1-Hydroxyethyl)anthraquinone

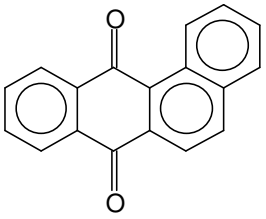

Benzanthracene-7,12-dione (**BAD**)

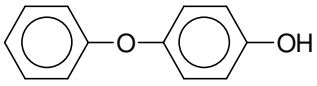

4-Phenoxyphenol

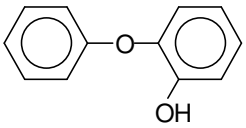

2-Phenoxyphenol

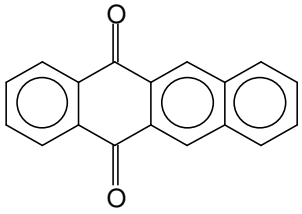

5,12-Naphthacenequinone (**NQ**)

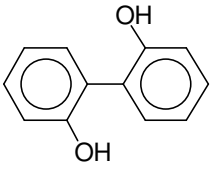

2,2'-Dihydroxybiphenyl

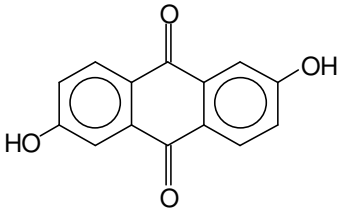

2,6-Dihydroxyanthraquinone (**DAQ**)

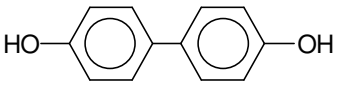

4,4'-Dihydroxybiphenyl

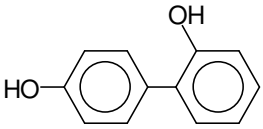

2,4'-Dihydroxybiphenyl

Scheme ESI2. Structure of the quinoid compounds under investigation (left) and of the detected transformation intermediates, formed upon irradiation of EtAQ and phenol (right).

Optimised structures of AQ, DAQ and EtAQ

Figure ESI3, Figure ESI4 and Figure ESI5 show the gas-phase optimised structures of AQ, DAQ and EtAQ, respectively, in their ground state (S_0). The list of atomic bonds is reported in Tables ESI6, ESI7 and ESI8, respectively. The obtained geometries were confirmed by analytical calculation of frequencies. The structures are here reported with their corresponding atoms labels, to facilitate the description of the results of our computational study.

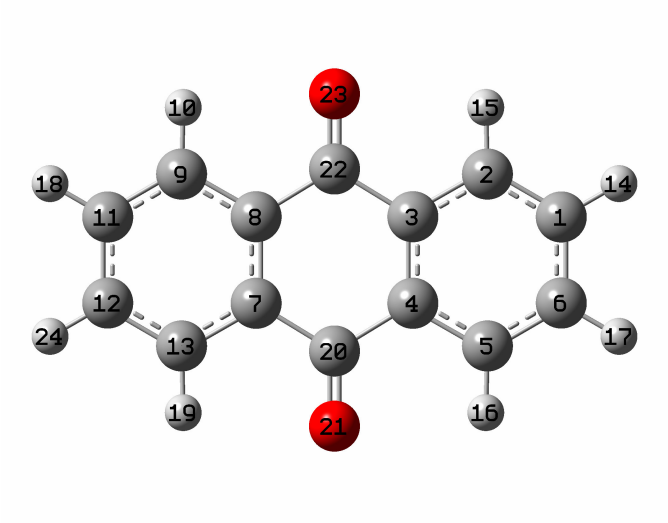

Figure ESI3. Optimised structure of AQ in its ground state (S_0).

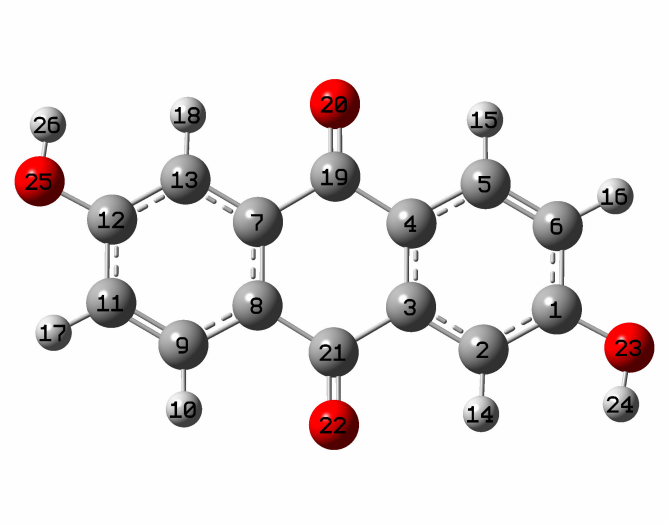

Figure ESI4. Optimised structure of DAQ in its ground state (S_0).

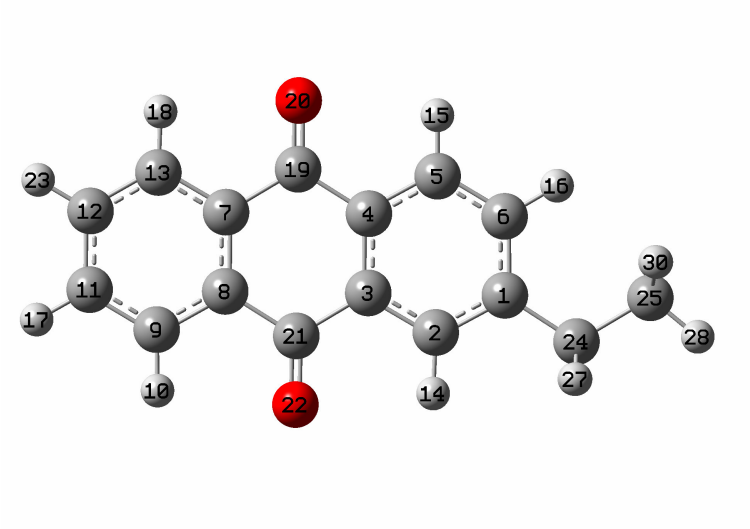

Figure ESI5. Optimised structure of EtAQ in its ground state (S_0).

A geometry optimisation has been carried out for AQ, EtAQ and DAQ in their lower-lying triplet state (T_1). A comparison of the bond lengths of the S_0 and T_1 states allows a better understanding of the nature of the T_1 states.

For the AQ molecule, an increase of the C=O bond length is noticed when passing from S_0 to T_1. In particular, the bond between the C22 – O23 atoms shows a noticeable lengthening of 0.08 Å, which confirms the incipient nature of the >C–O$^{\bullet}$ bond at the excited state. The other carbonyl group (C20 – O21 atoms) displays just a weak lengthening (0.01 Å), similarly to the C–C lengths of the two lateral aromatic rings. As a consequence of the C=O lengthening there is a shortening of the C–C bond in the α position with respect to the carbonyl group, which is more marked for the C3 – C22 – C8 system where the adjacent carbonyl stretching is more evident. The C–H bonds show negligible modifications. Information regarding AQ bond lengths is reported in Table ESI6.

The DAQ molecule has two -OH substituents and this leads to a change in its symmetry (from D_{2h} of AQ to C_{2h} of DAQ). The six-member carbon ring (C1 to C6) is poorly involved in spin resonance. Consequently, its aromaticity and bond lengths are almost the same as those in the S_0 state, and the distance between the C1 – O23 atoms remains unperturbed. Also in this case, as for AQ, a lengthening of the C=O bonds is noticed. One carbonyl group (C21 – O22) shows a higher increase in interatomic distance than the other one (C19 – O20), *i.e.* 0.035 *vs.* 0.020 Å. To counterbalance the lengthening of the C=O bonds, a shrinking of the central six-member ring of the molecule is observed. The C-C bonds in α with respect to the carbonyl group tend to gain a more marked sp^2 character. This phenomenon is particularly intense for the C8 – C21 bond, showing a decrease of 0.052 Å. This could be interpreted in terms of both adjustment of the DAQ atoms in their new settlement for the $S_0 \rightarrow T_1$ transition, and as consequence of the new resonance system occurring on the left side of the molecule, *i.e.* the conjugation between the -OH group and the dienic portion of the ring. For this reason the six-member carbon ring (C7 to C13) evolves from a phenolic-type into a quinoid-type structure, adjusting remarkably some bond lengths (C7 – C8, C8

– C9 and C11 – C12 show an increase of 0.065, 0.037 and 0.050 Å, respectively). The C12 – O25 bond is shortened due to spin resonance (0.016 Å), confirming the incipient nature of the >C–O$^{\bullet}$ bond at the excited state (see Figure 9 in the manuscript for a pictorial scheme of these effects). Information regarding DAQ bond lengths is reported in Table ESI7.

The EtAQ molecule (C_S symmetry), when passing from S_0 to T_1, shows the same bond length changes of AQ, namely the marked lengthening of the C21-O22 carbonyl group and the shortening of the C–C bonds in the α position with respect to the cited carbonyl group (C3-C21-C8 system).

Table ESI 6. Bond lengths of the optimised AQ geometry in its S_0 and T_1 states.

Bond length (Å)	**AQ (S_0)**	**AQ (T_1)**
C22 – O23	1.2193	1.3014
C20 – O21	1.2193	1.2308
C1 – C2	1.3892	1.3792
C2 – C3	1.3976	1.4156
C3 – C4	1.4058	1.4156
C4 – C5	1.3978	1.4026
C5 – C6	1.3893	1.3834
C6 – C1	1.3975	1.4061
C7 – C8	1.4057	1.4156
C8 – C9	1.3977	1.4156
C9 – C11	1.3893	1.3792
C11 – C12	1.3974	1.4061
C12 – C13	1.3893	1.3834
C13 – C7	1.3979	1.4026
C7 – C20	1.4926	1.4770
C20 – C4	1.4926	1.4771
C3 – C22	1.4927	1.4410
C22 – C8	1.4926	1.4410
C1 –H14	1.0841	1.0841
C2 – H15	1.0829	1.0836
C5 – H16	1.0829	1.0834
C6 – H17	1.0841	1.0837
C9 – H10	1.0830	1.0836
C11 – H18	1.0841	1.0841
C12 – H24	1.0838	1.0836
C13 – H19	1.0830	1.0834

Mulliken atomic spin densities of AQ in its T_1 state:

1	C	-0.060777
2	C	0.128816
3	C	-0.010696
4	C	0.138971
5	C	-0.050138
6	C	0.124872
7	C	0.138955
8	C	-0.010683
9	C	0.128824
10	H	-0.006734
11	C	-0.060772
12	C	0.124853
13	C	-0.050131
14	H	0.003207
15	H	-0.006734
16	H	0.002598
17	H	-0.007178
18	H	0.003206
19	H	0.002598
20	C	-0.013835
21	O	0.203419
22	C	0.322594
23	O	0.961942
24	H	-0.007177

Sum of Mulliken spin densities= 2.00000

Table ESI 7. Bond lengths of the optimised DAQ geometry in its S_0 and T_1 states.

Bond length (Å)	**DAQ (S_0)**	**DAQ (T_1)**
C21 – O22	1.2212	1.2567
C19 – O20	1.2212	1.2412
C12 – O25	1.3578	1.3414
C1 – O23	1.3578	1.3565
C1 – C2	1.3940	1.3870
C2 – C3	1.3927	1.4008
C3 – C4	1.4052	1.4199
C4 – C5	1.4014	1.4141
C5 – C6	1.3830	1.3729
C6 – C1	1.4027	1.4148
C7 – C8	1.4051	1.4702
C8 – C9	1.4014	1.4384
C9 – C11	1.3829	1.3539
C11 – C12	1.4027	1.4528
C12 – C13	1.3940	1.3919
C13 – C7	1.3927	1.3877
C7 – C19	1.4972	1.4605
C19 – C4	1.4816	1.4686
C3 – C21	1.4972	1.4681
C21 – C8	1.4916	1.4397
C2 –H14	1.0851	1.0851
C5 – H15	1.0829	1.0829
C6 – H16	1.0831	1.0831
C9 – H10	1.0829	1.0822
C11 – H17	1.0831	1.0827
C13 – H18	1.0851	1.0862
O25 – H26	0.9635	0.9669
O23 – H24	0.9635	0.9642

Mulliken atomic spin densities of DAQ in its T_1 state:

1	C	0.054797
2	C	0.019617
3	C	0.031226
4	C	0.074356
5	C	0.001478
6	C	0.025466
7	C	0.239933
8	C	0.477089
9	C	-0.051240
10	H	-0.000880
11	C	0.162017
12	C	0.303870
13	C	-0.029262
14	H	-0.002232
15	H	-0.001106
16	H	-0.001740
17	H	-0.010192
18	H	-0.000545
19	C	0.010684
20	O	0.198101
21	C	0.003797
22	O	0.339950
23	O	0.031433
24	H	-0.001075
25	O	0.128799
26	H	-0.004338

Sum of Mulliken spin densities = 2.00000

Table ESI 8. Bond lengths of the optimised EtAQ geometry in its S_0 and T_1 states.

Bond length (Å)	**EtAQ (S_0)**	**EtAQ (T_1)**
C19 – O20	1.2199	1.2307
C21 – O22	1.2195	1.3018
C1 – C2	1.3982	1.3878
C2 – C3	1.3931	1.4113
C3 – C4	1.4070	1.4150
C4 – C5	1.3946	1.3992
C5 – C6	1.3905	1.3848
C6 – C1	1.4010	1.4095
C7 – C8	1.4058	1.4159
C8 – C9	1.3978	1.4160
C9 – C11	1.3892	1.3791
C11 – C12	1.3974	1.4062
C12 – C13	1.3892	1.3835
C13 – C7	1.3976	1.4024
C7 – C19	1.4936	1.4778
C19 – C4	1.4886	1.4758
C3 – C21	1.4926	1.4429
C21 – C8	1.4931	1.4405
C1 – C24	1.5178	1.5204
C24 – C25	1.5293	1.5297
C2 –H14	1.0845	1.0852
C5 – H15	1.0831	1.0837
C6 – H16	1.0829	1.0824
C9 – H10	1.0829	1.0837
C11 – H17	1.0841	1.0842
C12 – H23	1.0841	1.0837
C13 – H18	1.0829	1.0835
C24 – H27	1.0964	1.0962
C24 – H26	1.0964	1.0963
C25 – H28	1.0923	1.0925
C25 – H29	1.0935	1.0934
C25 – H30	1.0935	1.0934

Mulliken atomic spin densities of EtAQ in its T_1 state:

1	C	-0.060249
2	C	0.141648
3	C	-0.009334
4	C	0.126028
5	C	-0.047859
6	C	0.116174
7	C	0.144022
8	C	-0.014204
9	C	0.1328
10	H	-0.006957
11	C	-0.062876
12	C	0.130034
13	C	-0.053144
14	H	-0.007486
15	H	0.002573
16	H	-0.006655
17	H	0.0033
18	H	0.002717
19	C	-0.013188
20	O	0.19661
21	C	0.330766
22	O	0.961032
23	H	-0.007484
24	C	0.004879

25	C	-0.000136
26	H	-0.001614
27	H	-0.001613
28	H	0.000069
29	H	0.000073
30	H	0.000073

Sum of Mulliken spin densities = 2.00000

Table ESI 9. Adiabatic (T_O) and vertical (T_V) transition energies of AQ, DAQ and EtAQ for the S_0-T_1 transition.

	AQ	***EtAQ***	***DAQ***
$\mathbf{T_O}$	2.57	2.59	2.52
$\mathbf{T_V}$	2.75	2.78	2.79

Energies are expressed in eV. Adiabatic energy is measured computing the difference among the two optimised geometries in the S_0 and T_1 states. Instead, vertical energy is calculated among the optimized geometry in the S_0 state and that at the T_1 state, constrained to S_0 (as reported in the following pictorial scheme).